Aliphatic Carbonyl Compounds (C_8-C_{26}) in Wintertime Atmospheric Aerosol in London, UK

Ruihe Lyu[1,2], Mohammed Salim Alam[1], Christopher Stark[1]

Ruixin Xu[1], Zongbo Shi[1], Yinchang Feng[2] and Roy M. Harrison[†*1]

[1] Division of Environmental Health and Risk Management

School of Geography, Earth and Environmental Sciences, University of Birmingham Edgbaston, Birmingham B15 2TT, UK

[2] State Environmental Protection Key Laboratory of Urban Ambient Air Particulate Matter Pollution Prevention and Control, College of Environmental Science and Engineering

Nankai University, Tianjin 300350, China

† Also at: Department of Environmental Sciences / Centre of Excellence in Environmental Studies, King Abdulaziz University, PO Box 80203, Jeddah, 21589, Saudi Arabia.

Corresponding authors:
E-mail: r.m.harrison@bham.ac.uk (Roy M. Harrison)

ABSTRACT

Three groups of aliphatic carbonyl compounds, the n-alkanals (C_8-C_{20}), n-alkan-2-ones (C_8-C_{26}) and n-alkan-3-ones (C_8-C_{19}) were measured in both particulate and vapour phases in air samples collected in London from January-April 2017. Four sites were sampled including two roof-top background sites, one ground-level urban background site and a street canyon location on Marylebone Road in central London. The n-alkanals showed the highest concentrations followed by the n-alkan-2-ones and the n-alkan-3-ones, the latter having appreciably lower concentrations. It seems likely that all compound groups have both primary and secondary sources and these are considered in the light of published laboratory work on the oxidation products of high molecular weight n-alkanes. All compound groups show relatively low correlation with black carbon and NOx in the background air of London, but in street canyon air heavily impacted by vehicle emissions, stronger correlations emerge especially for the n-alkanals. It appears that vehicle exhaust is likely to be a major contributor for concentrations of the n-alkanals whereas it is a much smaller contributor to the n-alkan-2-ones and n-alkan-3-ones. Other primary sources such as cooking or wood burning may be contributors for the ketones but were not directly evaluated. It seems likely that there is also a significant contribution from photo-oxidation of n-alkanes and this would be consistent with the much higher abundance of the n-alkan-2-ones relative to the n-alkan-3-ones if the formation mechanism were to be through oxidation of condensed phase alkanes. Vapour-particle partitioning fitted the Pankow model well for the n-alkan-2-ones but less well for the other compound groups, although somewhat stronger relationships were seen at the Marylebone Road site than at the background sites. The former observation gives support to the n-alkane-2-ones being a predominantly secondary product, whereas primary sources of the other groups are more prominent.

Keywords: Carbonyl compounds; n-alkanals; n-alkan-2-ones; n-alkan-3-ones; organic aerosol; partitioning;

1. INTRODUCTION

Carbonyl compounds are classified as polar organic compounds, constituting a portion of the oxygenated organic compounds in atmospheric particulate matter (PM). Aliphatic carbonyl compounds are directly emitted into the atmosphere from primary biogenic and anthropogenic sources (Schauer et al., 2001, 2002a, b), as well as being secondary products of atmospheric oxidation of hydrocarbons (Chacon-Madrid et al., 2010; Zhang et al., 2015; Han et al., 2016).

The most abundant atmospheric carbonyls are methanal (formaldehyde) and ethanal (acetaldehyde), and many studies have described their emission sources and chemical formation in urban and rural samples (Duan et al., 2016). Long-chain aliphatic carbonyl compounds have been identified in PM and reported in few published papers (Gogou et al., 1996; Andreou and Rapsomanikis, 2009), and these compounds are considered to be formed from atmospheric oxidation processes affecting biogenic emissions of alkanes. Anthropogenic activity is also considered to be a significant contributor to the aliphatic carbonyls. Appreciable concentrations of aliphatic carbonyl compounds have been identified in emissions from road vehicles (Schauer et al., 1999a; 2002b), coal combustion (Oros and Simoneit, 2000), wood burning (Rogge et al., 1998) and cooking processes (Zhao et al., 2007a,b), spanning a wide range of molecular weights. Furthermore, chamber studies (Chacon-Madrid and Donahue, 2011; Algrim and Ziemann, 2016) have demonstrated that the aliphatic carbonyl compounds are very important precursors of secondary organic aerosol (SOA) when they react with OH radicals in the presence of NO_x.

The oxidation of n-alkanes by hydroxyl radical is considered to be an important source of aliphatic carbonyl compounds. It was believed that the n-alkanals with carbon atoms numbering less than 20 indicate oxidation of alkanes, whereas the higher compounds were usually considered to be of direct biogenic origin (Rogge et al., 1998). The homologues and isomers of n-alkanals and n-alkanones have been identified as OH oxidation products of n-alkanes in many chamber and flow tube studies (Zhang et al., 2015; Schilling Fahnestock et al., 2015; Ruehl et al., 2013; Yee et al., 2012), although not all studies identified the position of the carbonyl group. The commonly accepted oxidation pathways of n-alkanes generally divide into functionalization and fragmentation. Functionalization occurs when an oxygenated functional group (–ONO_2, –OH, –C=O, –C(O)O– and –OOH) is added to a molecule, leaving the carbon skeleton intact. Alternatively, fragmentation involves C−C bond cleavage and produces two oxidation products with smaller carbon numbers than the reactant. The chamber studies of dodecane oxidation include observations of aldehydes and ketones as oxidation products (Schilling Fahnestock et al., 2015; Yee et al., 2012).

In London, with a high population density and a large number of diesel engine vehicles, the aliphatic hydrocarbons constitute an important fraction of ambient aerosols. Anthropogenic activities and secondary formation contribute to the emission and production of carbonyl compounds within the city. The objectives of the present study were the identification and quantification of aliphatic carbonyl compounds in particle and vapour samples collected in London from January to April 2017. This work has aided an understanding of the concentrations and secondary formation of carbonyls in the London atmosphere. Spatial and temporal variations of the studied carbonyl compounds were assessed and used to infer sources. One of the main objectives was to provide gas/particle partitioning

coefficients of identified carbonyls under realistic conditions. Diagnostic criteria were used to estimate the sources of identifiable atmospheric carbonyl compounds. Additionally, for the first time, concentrations of particulate and gaseous n-alkan-3-ones are reported.

2. MATERIALS AND METHODS

2.1 Sampling Method and Site Characteristics

Three sampling campaigns were carried out between 23 January and 18 April 2017 at four sampling sites (Figure 1) in London. The first campaign used two sampling sites, one located on the roof of a building (15 m above ground) of the Regent's University (51°31′N, -0°9′W), hereafter referred to as RU, sampled from 23 January 2017 to 19 February 2017, the other located on the roof (20 m above ground) of a building which belongs to the University of Westminster on the southern side of Marylebone Road (hereafter referred to as WM), sampled from 24 January 2017 to 20 February 2017. The third sampling site was located at ground level at Eltham (51°27′N, 0°4′E), hereafter referred to as EL, sampled from 23 February 2017 to 21 March 2017, which is located in suburban south London, and the fourth sampling site was located at ground level on the southern side of Marylebone Road (51°31′N, -0°9′W), hereafter referred to as MR, sampled from 22 March 2017 to 18 April 2017. Marylebone Road is in London's commercial centre, and is an important thoroughfare carrying 80-90,000 vehicles per day through central London. The Regent's University site is within Regent's Park to the north of Marylebone Road. The Eltham site is in a typical residential neighbourhood, 22 km from the MR site. Earlier work at the Marylebone Road and a separate Regent's Park site is described by Harrison et al. (2012).

115 The particle samples were collected on polypropylene backed PTFE filters (47 mm, Whatman) which
116 preceded stainless steel sorbent tubes packed with 1cm quartz wool, 300 mg Carbograph 2TD 40/60
117 (Markes International, Llantrisant, UK) and sealed with stainless-steel caps before and after sampling.
118 Sampling took place for sequential 24-hour periods at a flow rate of 1.5 L min^{-1} using an in-house
119 developed automated sampler. Field blank filters and sorbent tubes were prepared for each site, and
120 recovery efficiencies were evaluated. Adsorption tube breakthrough was tested in the field with six
121 replicates of two tubes in series and for compounds of ≥ C_{11} recovery exceeded 95% on the first tube.
122 It was 85% for the C_{10} compounds, and lower for C_9 and C_8 for which data are not reported. After
123 the sampling, each filter was placed in a clean sealed petri dish, wrapped in aluminium foil and stored
124 in the freezer at -18ºC prior to analysis. Black carbon (BC) was simultaneously monitored during the
125 sampling period at RU and WM sites using an aethalometer (Model AE22, Magee Science).
126 Measurements of BC and NO_x at MR and NO_x at EL were provided by the national network sites of
127 Marylebone Road, and Eltham (https://uk-air.defra.gov.uk/).

128

129 **2.2 Analytical Instrumentation**

130 The particle samples were analyzed using a 2D gas chromatograph (GC, 7890A, Agilent
131 Technologies, Wilmington, DE, USA) equipped with a Zoex ZX2 cryogenic modulator (Houston,
132 TX, USA). The first dimension was equipped with a SGE DBX5, non-polar capillary column (30.0
133 m, 0.25 mm ID, 0.25 mm – 5.00% phenyl polysilphenylene-siloxane), and the second-dimension
134 column equipped with a SGE DBX50 (4.00 m, 0.10 mm ID, 0.10 mm – 50.0% phenyl
135 polysilphenylene-siloxane). The GC × GC was interfaced with a Bench-ToF-Select, time-of-flight
136 mass spectrometer (ToF-MS, Markes International, Llantrisant, UK). The acquisition speed was 50.0

Hz with a mass resolution of >1200 fwhm at 70.0 eV and the mass range was 35.0 to 600 m/z. All data produced were processed using GC Image v2.5 (Zoex Corporation, Houston, US).

2.3 Analysis of Samples

Standards used in these experiments included 19 alkanes, C_8 to C_{26} (Sigma-Aldrich, UK, purity >99.2%); 12 n-aldehydes, C_8 to C_{13} (Sigma-Aldrich, UK, purity ≥95.0%), C_{14} to C_{18} (Tokyo Chemical Industry UK Ltd, purity >95.0%); and 10 2-ketones, C_8 to C_{13} and C_{15} to C_{18} (Sigma-Aldrich, UK, purity ≥98.0%) and C_{14} (Tokyo Chemical Industry UK Ltd, purity 97.0%).

The filters were spiked with 30.0 µL of 30.0 µg mL^{-1} deuterated internal standards (dodecane-d_{26}, pentadecane-d_{32}, eicosane-d_{42}, pentacosane-d_{52}, triacontane-d_{62}, butylbenzene-d_{14}, nonylbenzene-2,3,4,5,6-d_5, biphenyl-d_{10}, p-terphenyl-d_{14}; Sigma-Aldrich, UK) for quantification and then immersed in dichloromethane (DCM), and ultra-sonicated for 20.0 min at 20.0ºC. The extract was filtered using a clean glass pipette column packed with glass wool and anhydrous Na_2SO_4, and concentrated to 50.0 µL under a gentle flow of nitrogen for analysis using GC × GC-ToF-MS. 1 µL of the extracted sample was injected in a split ratio 100:1 at 300ºC. The initial temperature of the primary oven (80.0ºC) was held for 2.0 min and then increased at 2.0 ºC min^{-1} to 210ºC, followed by 1.5 ºC min^{-1} to 325 ºC. The initial temperature of the secondary oven (120ºC) was held for 2.0 min and then increased at 3.0ºC min^{-1} to 200ºC, followed by 2.00ºC min^{-1} to 300ºC and a final increase of 1.0ºC min^{-1} to 330 ºC to ensure all species passed through the column. The transfer line temperature was 330 ºC and the ion source temperature was 280ºC. Helium was used as the carrier

gas at a constant flow rate of 1.0 mL min^{-1}. Further details of the instrumentation and data processing methods is given by Alam et al. (2016a,b).

The sorbent tubes were analyzed by an injection port thermal desorption unit (Unity 2, Markes International, Llantrisant, UK) and subsequently analyzed using GC × GC-ToF-MS. Briefly, the tubes were spiked with 1 ng of deuterated internal standard for quantification and desorbed onto the cold trap at 350ºC for 15.0 min (trap held at 20.0ºC). The trap was then purged onto the column in a split ratio of 100:1 at 350ºC and held for 4.0 min. The initial temperature of the primary oven (90.0ºC) was held for 2.0 min and then increased to 2.0ºC min^{-1} to 240ºC, followed by 3.0ºC min^{-1} to 310ºC and held for 5.0 min. The initial temperature of the secondary oven (40.0ºC) was held for 2.0 min and then increased at 3.0ºC min^{-1} to 250ºC, followed by an increase of 1.5ºC min^{-1} to 315ºC and held for 5.0 min. Helium was used as carrier gas for the thermally desorbed organic compounds, with a gas flow rate of 1.0 mL min^{-1}.

Qualitative analysis

Compound identification was based on the GC×GC-TOFMS spectra library, NIST mass spectral library and in conjunction with authentic standards. Compounds within the homologous series for which standards were not available were identified by comparing their retention time interval between their homologues, and by comparison of mass spectra to the standards for similar compounds within the series, by comparison to the NIST mass spectral library and by the analysis of fragmentation patterns.

Quantitative analysis

An internal standard solution (outlined above) was added to the samples to extract prior to instrumental analysis. Five internal standards (pentadecane-d_{32}, eicosane-d_{42}, pentacosane-d_{52}, triacontane-d_{62}, nonylbenzene-2,3,4,5,6-d_5) were used in the calculation of carbonyl compound concentrations.

The quantification for alkanes, aldehydes and 2-ketones was performed by the linear regression method using seven-point calibration curves (0.05, 0.10, 0.25, 0.50, 1.00, 2.00, 3.00 ng μL^{-1}) established between the authentic standards/internal standard concentration ratios and the corresponding peak area ratios. The calibration curves for all target compounds were highly linear (r^2>0.99, from 0.990 to 0.997), demonstrating the consistency and reproducibility of this method. Limits of detection for individual compounds were typically in the range 0.04–0.12 ng m^{-3}. 3-ketones were quantified using the calibration curves for 2-ketones. This applicability of quantification of individual compounds using isomers of the same compound functionality (which have authentic standards) has been discussed elsewhere and has a reported uncertainty of 24% (Alam et al., 2018). Alkan-2-ones and alkan-3-ones were not well separated by the chromatography. These were separated manually using the peak cutting tool, attributing fragments at m/z 58 and 71 to 2-ketones and m/z 72 and 85 to 3-ketones.

Field and laboratory blanks were routinely analysed to evaluate analytical bias and precision. Blank levels of individual analytes were normally very low. Recovery efficiencies were determined by analyzing the blank samples spiked with standard compounds. Mean recoveries ranged between 78.0

and 102%. All quantities reported here have been corrected according to their recovery efficiencies. Detection limits are reported in Table S1.

3. RESULTS AND DISCUSSION

3.1 Mass Concentration of Particle-Bound Carbonyl Compounds

The study of temporal and spatial variations of air pollutants can provide valuable information about their sources and atmospheric processing. The time series of particle-bound n-alkanals, n-alkan-2-ones, and n-alkan-3-ones are plotted in Figure 2. It is clear that the concentrations of n-alkanals varied substantially with date, and were always higher than n-alkanones at four sites. It is also clear from Figure 3 that concentrations were broadly similar at the background sites, RU, WM and EL, but are elevated, especially for the n-alkanals, at MR. This is strongly indicative of a road traffic source.

Carbonyls including n-alkanone homologues could result as fragmentation products from larger alkane precursors during gas-phase oxidation (Yee et al., 2012; Schilling Fahnestock et al., 2015) or as functionalized products from heterogeneous oxidation of particle-bound alkanes (Ruehl et al., 2013; Zhang et al., 2015). While carbonyl compounds are expected to be amongst first generation oxidation products of alkanes, product yields are not well known, and are highly dependent upon the chemical environment in which oxidation occurs. Yee et al. (2012) show substantial yields of mono-carbonyl product, the position of substitution undefined, in the low-NO_x oxidation of n-dodecane. Ruehl et al. (2013) report the production of 2- through 14-octacosanone from the oxidation of octacosane, giving relative, but not absolute yields. Schilling Fahnestock et al. (2014) report

oxidation products of dodecane formed in both low-NO and high NO environments (<d.l and NO = 97.5 ppb respectively). A singly substituted unfragmented ketone product is reported only from the low-NO oxidation, and in relatively low yield amongst many products. Lim and Ziemann (2009) propose a reaction scheme for the OH-initiated oxidation of alkanes in the presence of NO_x. They express the view that first generation carbonyl formation is negligible at high NO concentrations for linear alkanes with C_n>6 since reactions of an alkoxy radical with O_2 are to slow to compete with isomerisation, which leads ultimately to hydroxynitrate and hydroxycarbonyl products. Ziemann (2011) also shows a substantial yield of alkylnitrates from OH-initiated oxidation of n-alkanes from C_{10}-C_{25} in the presence of NO. The NO concentrations in the background air of London are <12 ppb typically (UK-Air, 2018), and hence lie between the low and high NO environments of experiments in the literature, therefore most probably permitting some oxidation to proceed through pathways leading to first generation carbonyl products.

Figure 3 shows the average total concentrations of particle-bound 1-alkanals, n-alkan-2-ones, and n-alkan-3-ones from January to April at four measurement sites, and the particle and gaseous phase concentrations are detailed in the Table S2 (Supporting Information). Total n-alkanals was defined as the sum of particle-bound n-alkanals ranging from C_8 to C_{20}. The particulate n-alkanals at the MR site accounted for 75.2% of the measured particle carbonyls with the average total concentration of 682 ng m^{-3}, and concentrations at the other sites were 167 ng m^{-3} at EL, 117 ng m^{-3} at WM and 82.6 ng m^{-3} at RU, accounting for 57.0%, 57.9% and 56.3% of the measured particulate carbonyls, respectively. The n-alkanals identified in this study differed substantially from those previously reported in samples collected from Crete (Gogou et al., 1996) and Athens (Andreou and

245 Rapsomanikis, 2009) in Greece. The n-alkanals from London presented narrower ranges of carbon
246 numbers and a higher concentration than rural and urban samples from Crete. The concentrations of
247 n-alkanal homologues (C_8-C_{20}) ranged from 5.50 to 141 ng m^{-3} (average 52.0 ng m^{-3}) at MR which
248 were far higher than 1.48-28.6 ng m^{-3} (average 6.44 ng m^{-3}) at RU, 1.42-50.3 ng m^{-3} (average 9.03
249 ng m^{-3}) at WM and 3.29-53.0 ng m^{-3} (average 13.0 ng m^{-3}) at EL (Table S1), unlike Crete where the
250 concentrations were 0.9-3.7 ng m^{-3} in rural (C_{15}-C_{30}) and 5.4-6.7 ng m^{-3} in urban (C_9-C_{22}) samples,
251 and the average concentration of all four sites was much higher than the 0.91 ng m^{-3} measured in
252 Athens (Andreou and Rapsomanikis, 2009) (C_{13}-C_{20}). This is a clear indication of a road traffic,
253 most probably diesel source which is greater in London. Earlier work has clearly demonstrated a
254 substantial elevation in traffic-generated pollutants at the Marylebone Road site, relative to
255 background sites within London (Harrison and Beddows, 2017).

256

257 As part of the CARBOSOL project (Oliveira et al., 2007), air samples were collected in summer and
258 winter at six rural sites across Europe. The particulate n-alkanals ranged from C_{11} to C_{30} with average
259 total concentrations between 1.0 ng m^{-3} and 19.0 ng m^{-3}, with higher concentrations in summer than
260 winter at all but one site. Maximum concentrations at all sites were in compounds >C_{22} indicating a
261 source from leaf surface abrasion products and biomass burning (Simoneit et al., 1967; Gogou et al.,
262 1996). This far exceeds the C_{max} (carbon number of the most abundant homologue) values seen in
263 the particulate fraction at our sites.

264

265 The n-alkan-2-one homologues measured in London ranged from C_8 to C_{26}, and the average total
266 particulate fraction concentration was 58.5 ng m^{-3} at RU, 75.1 ng m^{-3} at WM, 112 ng m^{-3} at EL and

186 ng m^{-3} at MR, approximately accounting for 39.9% (RU), 37.0% (WM), 38.1% (EL) and 20.5% (MR) of the total particulate carbonyls, respectively (Figure 3). The published data from Greece indicated that the concentrations of n-alkan-2-ones were independent of the seasons, and an average of 5.40 ng m^{-3} (C_{13}-C_{29}) was measured in August and 5.44 ng m^{-3} in March at Athinas St, but 12.88 ng m^{-3} was measured in March at the elevated (20 m) AEDA site in Athens (Gogou et al., 1996). Concentrations in Crete for alkan-2-ones (C_{10}-C_{31}) were 0.4-2.1 ng m^{-3} at the rural site and 1.9-2.6 ng m^{-3} at the urban site (Andreou and Rapsomanikis, 2009). The CARBOSOL project also determined concentrations of n-alkan-2-ones, between C_{14} and C_{31} with a C_{max} at C_{28} or C_{29} at all but one site. Average concentrations ranged from 0.15 ng m^{-3} (C_{17-29}) to 3.35 (C_{14}-C_{31}), very much below the concentrations at our London sampling site. Cheng et al. (2006) measured concentrations of n-alkan-2-ones in the Lower Fraser Valley, Canada, in $PM_{2.5}$. Samples collected in a road tunnel showed the highest concentrations, total 1.8-12.6 ng m^{-3} for C_{10}-C_{31}, and were higher in daytime than nighttime. Concentrations at a forest site were 1.1-7.2 ng m^{-3} without a diurnal pattern. Values of C_{max} ranged from C_{16-17} at the road tunnel to C_{27} (secondary maximum) at the forest site. Values of CPI (Carbon Preference Index, defined in Section 3.2.1) averaged across sites from 1.00 to 1.34, giving little evidence for a substantial biogenic input from higher plant waxes. These data clearly suggest a road traffic source in London, but less influential than for the n-alkanals for which the increment at the roadside MR site is much greater.

The n-alkan-3-one homologues identified in the samples ranged from C_8 to C_{19}, and the average of individual compound concentrations was 0.52 ng m^{-3} at RU, 0.94 ng m^{-3} at WM, 1.37 ng m^{-3} at EL and 3.34 ng m^{-3} at MR. The concentrations of n-alkan-3-ones at the four sites were lower than the n-

alkanals and n-alkan-2-ones, and MR had the highest average total mass concentrations 39.4 ng m^{-3}, followed by 14.3 ng m^{-3} at EL, 10.4 ng m^{-3} at WM and 5.65 ng m^{-3} at RU, respectively.

The isomeric carbonyls formed via OH-initiated heterogeneous reactions of n-octacosane (C_{28}) exhibit a pronounced preference at the 2-position of the molecule chain (Ruehl et al., 2013). The n-octacosan-2-ones have the highest relative yield (1.00), followed by n-octacosan-3-ones (0.50), while other isomeric carbonyl yields were lower than 0.20. The same results were found in the subsequent chamber studies of n-alkanes (Zhang et al., 2015) (C_{20}, C_{22}, C_{24} but not C_{18}). The main probable reason was that a large fraction of C_{18} evaporated into the gas phase, and OH oxidation happened in the gas phase (homogeneous reaction). This may be supported by the evidence from previous studies (Kwok and Atkinson, 1995; Ruehl et al., 2013), which found that the isomeric distribution of oxidation products of n-alkanes depends upon whether the reaction occurs in the gas phase or at the particle surface (Kwok and Atkinson, 1995; Ruehl et al., 2013). The homogeneous gas-phase oxidation occurs fast, and H-abstraction by OH radicals occurs at all carbon sites. The fractions of the OH radical reaction by H atom abstraction from n-decane at the 1-, 2-, 3-, 4- and 5-positions are 3.10%, 20.7%, 25.4%, 25.4%, and 25.4%, respectively, and the products from gas phase (homogeneous) reaction were generally in accord with structure-reactivity relationship (SRR) predictions (Kwok and Atkinson, 1995; Aschmann et al., 2001). Zhang et al. (2015) report on the competition between homogeneous and heterogeneous oxidation of medium to high molecular weight alkanes. They express the view that in the atmosphere, compounds typically classified as semi-volatile evaporate sufficiently rapidly that homogeneous gas phase oxidation is more rapid than oxidation in the condensed phase.

311 During the field experiment, the n-alkanal homologues were abundant in all samples, and this is
312 probably attributable to the primary emission sources, including diesel vehicles (Schauer et al.,
313 1999a), gasoline cars (Schauer et al., 2002b), wood burning (Rogge et al., 1998) and cooking aerosol
314 (Schauer et al., 1999b). Correlations with other largely vehicle-generated pollutants (see later)
315 support this interpretation. The particulate form of the n-alkane homologues (C_{14}-C_{36}) identified in
316 the samples dominated for >C_{25} and there was a significant particulate fraction (>60%) for all but the
317 low MW n-alkanes (C_{14}-C_{18}) (unpublished data). The H-abstraction by OH radicals may therefore
318 have been dominated by heterogeneous reactions generating the higher concentrations of n-alkan-2-
319 ones than n-alkan-3-ones that were found in all samples. The ratio of n-alkan-2-ones/n-alkan-3-ones
320 (C_{11}-C_{18}) with the same carbon atom number ranged from 2.35-11.3 at four measurement sites.
321 Surprisingly, although the n-alkane (C_{11}-C_{13}) oxidation was expected to be dominated by
322 homogeneous gas phase reactions, the n-alkan-2-one/n-alkan-3-one ratios were still greater than 2.00.
323 The probable reason was that the lower molecular weight n-alkan-2-ones were significantly impacted
324 by primary emission sources such as cooking (Zhao et al., 2007a,b). Another possible reason is that
325 the n-alkan-2-one and n-alkan-3-one homologues with lower carbon atom numbers originated in part
326 from the fragmental products of higher n-alkanes (Yee et al., 2012; Schilling Fahnestock et al., 2015),
327 although fragmentation reactions would result mainly in the formation of alkanals, and are less likely
328 to occur than isomerisation leading mostly to multifunctional products.
329
330 The ratios of n-alkan-2-ones/n-alkanes, n-alkan-3-ones/n-alkanes (with same carbon numbers) were
331 calculated and are reported in Table S3. The n-alkan-3-ones with carbon numbers higher than C_{20}
332 were not identified in the samples, indicating that both the gas phase and heterogeneous reactions of

higher molecular weight n-alkanes were slow, the former probably due to the low vapour phase presence of n-alkanes. The ratios of n-alkan-3-ones/n-alkanes at four measurement sites gradually increased from $C_{11,}$ and then decreased from C_{17}, while higher ratios of n-alkan-2-ones/n-alkanes were observed in the range from C_{17} to C_{22}, probably indicating a shift from homogeneous gas phase reactions to heterogeneous reactions with the increase of carbon numbers. The low ratios of n-alkan-2-ones/n-alkanes with carbon numbers from C_{23} to C_{26} might be explained by the low diffusion rate from the inner particle to the surface with the increasing carbon number of n-alkanes, even though heterogeneous reactions would be the expected dominant pathway.

3.2 Sources of Carbonyl Compounds

3.2.1 Homologue distribution and carbon preference index (CPI)

Figure 4 shows the average concentrations, and molecular distributions of particle-bound carbonyl compounds at the four sites. The values of carbon preference index (CPI) were calculated to estimate the origin of carbonyl compounds, according to Bray and Evans (1961):

$$\mathrm{CPI} = \frac{1}{2}\left(\frac{\sum_4^m C_{2i+1}}{\sum_4^m C_{2i}} + \frac{\sum_4^m C_{2i+1}}{\sum_5^{m+1} C_{2i}}\right)$$

For n-alkanals and n-alkan-3-ones (m=9):$\mathrm{CPI} = \frac{1}{2}\left(\frac{\sum odd(C_9-C_{19})}{\sum even(C_8-C_{18})} + \frac{\sum odd(C_9-C_{19})}{\sum even(C_{10}-C_{20})}\right)$

For n-alkan-2-ones (m=12): $\mathrm{CPI} = \frac{1}{2}\left(\frac{\sum odd(C_9-C_{25})}{\sum even(C_8-C_{24})} + \frac{\sum odd(C_9-C_{25})}{\sum even(C_{10}-C_{26})}\right)$

where *i* takes values between 4 and *m*, and 5 and *m* as in the equation, and

m = 9 for n-alkanal and n-alkan-3-ones

354 m = 12 for n-alkan-2-ones

355 The carbon number of the homologue of highest concentration (C_{max}) can be indicative of the source.
356 Table. 1 presents the CPI and C_{max} of particle-bound carbonyl compounds calculated in the current
357 and other studies. A CPI of ≤1 is an indication of an anthropogenic source, while a CPI of 1-5
358 shows a mixture of anthropogenic and biogenic sources and a CPI >5 suggests a biogenic (plant wax)
359 source.

360

361 The n-alkanes which are potential precursors of the oxygenates described typically showed two C_{max}
362 values, the first at C_{13} (the lowest MW compound measured), and at C_{23}. The CPI values for the
363 n-alkanes were between 0.97-1.02 at the four measurements sites (unpublished data).

364

365 According to the low CPI (0.41-1.07) at the four sites, the n-alkanal homologues with carbon number
366 from C_8 to C_{20} mainly originate from anthropogenic emissions or OH oxidation of fossil-derived
367 hydrocarbons. The particle-bound n-alkanals exhibited a similar distribution of carbon number from
368 January to April at four sites, and they had the same C_{max} at C_8 with concentration 28.6 ng m^{-3} at
369 RU, 50.3 ng m^{-3} at WM, 53.0 ng m^{-3} at EL and 141 ng m^{-3} at MR, respectively. This compound may
370 be a fragmentation product, oxidation product or primary emission. In addition, the distribution of
371 n-alkanals had a second concentration peak at C_{15} (MR) and C_{18} (RU, WM, and EL). The C_{18}
372 compound was observed accounting for the highest percentage of the total mass of n-alkanals in
373 some rural aerosol samples (Gogou et al., 1996) in Crete. Andreou and Rapsomanikis reported the
374 C_{max} as C_{15} or C_{17} in Athens (Andreou and Rapsomanikis, 2009) and attributed this to the oxidation

of n-alkanes. However, a C_{max} at C_{26} or C_{28} in urban Crete (Gogou et al., 1996) was observed, suggestive of biogenic input. The homologue distribution and CPI of n-alkanals in this study differed from those previous reports, and demonstrated weak biogenic input and a strong impact of anthropogenic activities in the London samples.

In this study, n-alkan-2-ones have similar homologue distributions and C_{max} (C_{19} or C_{20}) (Table 2) at RU, WM and EL sites, and the total concentration from C_{16} to C_{23} accounts for 76.0%, 76.1% and 68.0% of ∑n-alkan-2-ones, respectively. The CPI values for n-alkan-2-ones ranged from 0.57 to 1.23 at the RU, MR and WM sites and were not indicative of major biogenic input, and were considered to mainly originate from anthropogenic activities and OH oxidation of anthropogenic n-alkanes. It is however notable that the CPI values for both the 2-ketones and 3-ketones exceed those for the alkanals (see Table 1), suggesting a contribution from contemporary biogenic sources, possibly wood smoke and cooking. At EL, the CPI of 1.57 is clearly indicative of a biogenic contribution in suburban south London. A difference was observed at the MR site, the n-alkan-2-ones with carbon atoms numbering from C_{12} to C_{18} accounting for 72.0% of ∑n-alkan-2-ones, with the C_{max} being at C_{16}. These data suggest a contribution of primary emissions from traffic at MR, but a dominant background, probably substantially secondary, at the other sites. The C_{max} of n-alkan-3-ones was at C_{16} at the MR site, at EL, C_{max} = C_{16}, WM, C_{max} = C_{17} and at RU, C_{max} = C_{17}, respectively.

3.2.2 The ratios of n-alkanes/n-alkanals

Diesel engine emission studies have been conducted previously in our group; details of the engine set up and exhaust sampling system are given elsewhere (Alam et al., 2016b). Briefly, the steady-state diesel engine operating conditions were at a load of 5.90 bar mean effective pressure (BMEP) and a speed of 1800 revolutions per minute (RPM), and samples (n=14) were collected both before a diesel oxidation catalyst (DOC) and after a diesel particulate filter (DPF). The n-alkanes (C_{12} - C_{37}) and 1-alkanals (C_9 - C_{18}) were quantified in the particle samples, while n-alkanones were not identified because their concentrations were lower than the limits of (detection 0.01–0.15 ng m^{-3}). The emission concentrations of n-alkanals ranged from 7.10 to 53.2 µg m^{-3} (before DOC) and 1.20 to 11.5 µg m^{-3} (after DPF), respectively, and the ratios of alkanes/alkanals (C_{13}-C_{18}) with the same carbon atom numbers ranged from 0.15 to 0.23 (before DOC) and 0.52 to 7.60 (after DPF). The n-alkane/n-alkanal (C_{13}-C_{18}) ratio at MR ranged from 0.30 to 5.7, while average ratios of 14.9 (RU), 11.5 (WM) and 14.7 (EL) were obtained, respectively. The similarity of the n-alkanes/n-alkanal ratio between MR and the engine studies (after DPF) strongly suggests that diesel vehicle emissions were the main source of alkanals at MR. The higher ratios at the other sites may be due to greater airmass aging and loss of alkanals due to their higher reactivity (Chacon-Madrid and Donahue, 2011; Chacon-Madrid et al., 2010).

The emission factors of total alkanes from diesel engines are reported to be 7 times greater than gasoline engines (Perrone et al., 2014), with n-alkanals with carbon atoms numbering lower than C_{11} being quantified in the exhaust from gasoline engines (Schauer et al., 2002b; Gentner et al., 2013). The n-alkane/n-alkanal (C_8-C_{10}) ratio with the same carbon numbers ranged from 5.60 to 14.3

418 (Schauer et al., 2002b), suggesting that gasoline combustion may be another potential source of
419 atmospheric n-alkanals.
420
421 **3.2.3 Correlation analysis**
422 Insights into the sources of carbonyls can be gained from intra-site correlation analysis with black
423 carbon (BC) and NO_x. This is more informative than comparisons between sites when sampling did
424 not take place simultaneously, as concentrations are strongly affected by weather conditions, making
425 inter-site comparisons difficult to interpret. In London, both black carbon and NO_x arise very
426 substantially from diesel vehicle emissions (Liu et al., 2014; Harrison et al., 2012; Harrison and
427 Beddows, 2017), and hence these are good measures of road traffic activity. The concentrations of
428 BC were simultaneously determined by the online instruments during the sampling periods, with the
429 average concentrations of 1.34, 1.94 and 3.58 μg m^{-3} at the RU, WM and MR sites, respectively.
430 The data for NO_x were provided by the national network sites, with the average concentrations of
431 23.4 and 202 μg m^{-3} at the EL and MR sites, respectively. At the MR site, the concentrations of BC
432 and NO_x averaged 5.00 μg m^{-3} and 281 μg m^{-3} when southerly winds were dominant compared to
433 2.60 and 128 μg m^{-3} for northerly winds. All correlations were carried out with the sum of particle
434 and vapour phases for the carbonyl compounds, and strong (r^2 = 0.87) and weak (r^2 = 0.12)
435 correlations between BC and NO_x were obtained when the southerly and northerly winds were
436 prevalent at MR, respectively. Marylebone Road is a street canyon site where a vortex circulation is
437 established by the wind. The effect is that on northerly wind sectors the sampling site on the southern
438 side of the road samples near-background air, while on southerly wind sectors, the traffic pollution
439 is carried to the sampling site, leading to elevated pollution levels affected heavily by the traffic

emissions. The strong correlation between BC and NO_x with southerly wind sectors is a reflection of their emission from road traffic. In addition, the correlations between n-alkanals (C_8-C_{20}) and BC, and between n-alkanals (C_8-C_{20}) and NO_x were calculated to assess the contribution of vehicular emissions (Table S4). The results showed that the correlations (r^2) between n-alkanals and BC gradually decreased from 0.61 (C_9) to 0.34 (C_{20}) at MR when the southerly winds were prevalent, indicating that the distribution of n-alkanals, and especially the lower MW compounds, was significantly impacted by the vehicular exhaust emissions. The average correlations at MR (southerly winds) between n-alkanals and BC, and between n-alkanals and NO_x were $r^2 = 0.47$ and $r^2 = 0.32$, respectively. These moderate correlations demonstrated that the vehicular emissions were a source of n-alkanals at MR, and contribute to the high background concentrations of n-alkanals in London. The other probable sources of n-alkanals include cooking emissions, wood burning, photooxidation of hydrocarbons and industrial emissions. Poorer correlations between n-alkanals and BC (average $r^2 = 0.15$), and between n-alkanals and NO_x (average $r^2 = 0.15$) were observed at MR in the north London background air sampled when northerly winds were prevalent. There were very weak correlations (average $r^2 < 0.10$) between n-alkanals and BC, and between n-alkanals and NO_x at the RU, WM and EL sites, which may be attributable to the high chemical reactivity of n-alkanals. High concentrations of furanones (γ-lactones) are generated via the photo-oxidation reaction of n-alkanals (Alves et al., 2001), and the total concentrations (particle and gas) were up to 376, 279, 347 and 318 ng m^{-3} at RU, WM, WL, and MR, respectively for the sum of furanone homologues (from 5-propyldihydro-2(3H)-furanone to 5-tetradecyldihydro-2(3H)-furanone).

461 The relationships (r^2 values) between BC and NO_x and the n-alkan-2-ones were low at all sites, but
462 notably higher with southerly winds at MR (average r^2 = 0.33 and 0.35 for BC and NO_x respectively)
463 than for northerly winds (r^2 = 0.16 and 0.03 respectively). This is strongly suggestive of a
464 contribution from vehicle exhaust to n-alkan-2-one concentrations, but smaller than that for n-
465 alkanals. In the case of the n-alkan-3-ones, correlations averaged r^2 = 0.25 with BC and r^2 = 0.21 for
466 NO_x in southerly winds, compared to r^2 = 0.08 and r^2 = 0.05 respectively for northerly winds. This
467 is also suggestive of a small, but not negligible contribution of vehicle emissions to n-alkan-3-ones.
468 The very low correlations observed in background air for both n-alkan-2-ones and n-alkan-3-ones
469 with BC and NO_x are suggestive of the importance of non-traffic sources, probably including
470 oxidation of n-alkanes. Both compound groups were below detection limit in the analyses of diesel
471 exhaust. The considerable predominance of n-alkan-2-one over n-alkan-3-one concentrations may
472 be indicative of a formation pathway from oxidation of condensed phase n-alkanes, but this is
473 speculative as primary emissions may be dominant.

474

475 **3.3 Gas and Particle Phase Partitioning**

476 The partitioning coefficient K_p between particles and vapour (≥ C_{10}) was calculated in this study
477 according to the following equation defined by Pankow (1994):

478

479 $$K_p = \frac{C_p}{C_g * TSP}$$

480

481 Where, C_p and C_g (μg m^{-3}) are the concentration of the compounds in the particulate phase and
482 gaseous phase, respectively. TSP is the concentration of total suspended particulate matter (μg m^{-3}),

which was estimated from the PM_{10} concentration (PM_{10}/TSP = 0.80), and daily average PM_{10} concentrations were taken from the national network sites (see Table S5). The partitioning coefficients K_p calculated from our data and the percentages in the particulate form are presented in Table 2. For the three types of carbonyls, the n-alkanals >C_{16}, n-alkan-2-ones >C_{19}, and n-alkan-3-ones > C_{18} the vapour concentrations were below detection limit, and the partitioning into the particulate phase gradually increased from C_8 to high molecular weight compounds.

Log Kp was regressed against vapour pressure (VP_T) for the relevant temperature derived from UManSysProp (http://umansysprop.seaes.manchester.ac.uk/) according to the following equation:

$$\text{Log } K_p = \text{m log}(VP_T) + b$$

The calculated log K_p versus log (VP_T) for the three types of carbonyls was calculated for each day, and the results appear in the Table S6. Data from four sites were over the temperature range 0.4–15.3 °C. A good fit to the data for n-alkan-2-ones (r^2 = 0.55–0.94 at RU, 0.64-0.93 at WM, 0.45-0.94 EL and 0.36-0.88 at MR) was obtained. It is notable that the fit to the regression equation as indicated by the r^2 value is appreciably higher at the MR site than at the other sites, especially in the case of the alkan-3-ones (Table S6). This is not easily explained, except perhaps by an increased particle surface area at the MR site which may enhance the kinetics of gas-particle exchange, leading to partitioning which is closer to equilibrium.

According to theory, the gradient of the plot of log K_P versus log (VP_T) should be -1 (Pankow, 1994). However, many measurement datasets for a number of semi-volatile compound groups including n-alkanes (Cincinelli et al., 2007; Karanasiou et al., 2007; Mandalakis et al., 2002) and PAH (Callen et al., 2008; Wang et al., 2011; Ma et al., 2011; Mandalakis et al., 2002) show a range of values, often around -0.5, but ranging to below -1, and in some cases positive. Callen et al., (2008) discuss the reasons for deviation from a value of -1, which include a lack of equilibrium, absorption into the organic matter (shallower than -0.6), adsorption processes (steeper than -1), and the averaging of conditions across a range of temperatures during a sampling period.

Our data for alkan-2-ones show high r^2 values and values of gradient (m) in the range of the literature for other groups of semi-volatile compounds. Average gradients at the four sites ranged from -0.46 to -0.26. The alkan-3-ones show generally considerably lower values of r^2 and average values of gradient at the four sites of -0.43 to -0.23. This poorer correlation could be the result of lower analytical precision. The n-alkanals show still lower values of r^2, and more variable and shallower values of slope. Mean slopes for the four sites ranged from -0.23 to -0.16. There were no positive daily values. The lower r^2 may be a result of disequilibrium for the alkanals which are dominated by primary emissions, and are also more reactive. It might also reflect a role for aqueous aerosol as an absorbing medium for these compounds containing a significant polar moiety, which would lead to deviations from the Pankow (1994) theory, and more variable behaviour as the availability of aqueous particles into which to partition would depend upon relative humidity, which is itself highly variable.

526 Samples were collected over 24-hour periods and hence the diurnal variation of temperature may be
527 relevant. Temperature data were taken from Heathrow Airport to the west of London and did not
528 show large diurnal fluctuations, so this should not be a major factor. The average diurnal
529 temperature range based upon hourly data was 6.9ºC.

530

531 The lower molecular weight n-alkanals show a much higher percentage in the condensed phase than
532 the ketone groups (Table 2).

533

534 This greater propensity to partition into the particles is unexpected, as the vapour pressures of the
535 alkanals are very similar to those of the ketones. It might possibly reflect a greater affinity of the
536 alkanals for solvation by water molecules, leading to increased partition into aqueous aerosol.

537

538 **4. CONCLUSIONS**

539 Three groups of carbonyl compounds were determined in the particle and gaseous phase in London
540 and concentrations are reported for n-alkanals (C_8-C_{20}), n-alkan-2-ones (C_8-C_{26}) and n-alkan-3-ones
541 (C_8-C_{19}). The Marylebone Road site has the highest concentration of particle-bound n-alkanals, and
542 the average total concentration was up to 682 ng m^{-3}, followed by 167 ng m^{-3} at EL, 117 ng m^{-3} at
543 WM and 82.6 ng m^{-3} at RU. The particulate n-alkanals were abundant in all samples at all four
544 measurement sites, accounting for more than 56.3% of total particle carbonyls. In addition, the
545 average total particle concentrations of n-alkan-2-ones and n-alkan-3-ones at four measurement sites
546 were in the range of 58.5-186 ng m^{-3} and 5.65-39.4 ng m^{-3}, respectively. Diagnostic criteria,

including molecular distribution, CPI, C_{max}, ratios and correlations, were used to assess the sources and their contributions to carbonyl compounds. The three groups of carbonyls have similar molecular distributions and C_{max} values at the four measurement sites, and their low CPI values (0.41-1.57) at the four sites indicate a weak biogenic input during sampling campaigns. Heavily traffic-influenced air and urban background air were measured at the MR site when southerly and northerly winds were prevalent respectively; correlations of r^2 = 0.47 and r^2=0.32 were obtained between n-alkanals and BC, and between between n-alkanals and NO_x, respectively in southerly winds. Vehicle emissions appear to be an important source of n-alkanals, which is confirmed by the similar ratios of n-alkanes/n-alkanals measured at MR (0.30-5.75) and in diesel engine exhaust studies (0.52-7.6), resulting in a high background concentration in London. In addition, the OH-initiated heterogeneous reactions of n-alkanes appear to be important sources of n-alkanones, even though weak contributions from vehicular exhaust emissions were suggested by correlation analysis with BC and NO_x in southerly winds at MR. Anthropogenic primary sources such as cooking (Abdullahi et al., 2013) may account for a proportion of the alkan-2-one and alkan-3-one concentrations measured in London, in addition to the secondary contribution from alkane oxidation. Any contribution from cooking or wood combustion is likely to be small, or the CPI would be greater.

In addition, the partitioning coefficients of carbonyls were determined from the relative proportions of the particle and gaseous phases of individual compounds, and generally showed a better fit at MR than at the other three sites. Fits to the Pankow (1994) model were best for alkan-2-ones and this most likely reflects the slow formation of the alkan-2-ones as secondary constituents, closer to phase

equilibrium than the predominantly emitted and more reactive alkanals which would be spatially more variable.

ACKNOWLEDGEMENTS

Primary collection of samples took place during the FASTER project which was funded by the European Research Council (ERC-2012-AdG, Proposal No. 320821). The authors would also like to thank the China Scholarship Council (CSC) for support to R.L., and the Natural Environment Research Council for support under the Air Pollution and Human Health (APHH) programme (NE/N007190/1).

AUTHOR CONTRIBUTIONS

RL performed the carbonyl compound calibrations, analysed the chromatograms and prepared a first draft of the paper. MSA and CS managed the analytical facility, ran the air sample analyses and provided preliminary interpretation. RX contributed alkane data. ZS and YF co-supervised the project which was conceived and led by RH who prepared final versions of the manuscript.

583 **REFERENCE**
584
585 Abdullahi, K.L., Delgado-Saborit, J.M., and R.M. Harrison: Emissions and indoor concentrations
586 of particulate matter and its specific chemical components from cooking: A review, Atmos.
587 Environ., 71, 260-294, http://dx.doi.org/10.1016/j.atmosenv.2013.01.061, 2013.
588
589 Alam, M. S., Stark, C., and Harrison, R. M.: Using variable ionization energy time-of-flight mass
590 spectrometry with comprehensive GC×GC to identify isomeric species, Anal. Chem., 88, 4211-
591 4220, http://www.doi.org/10.1021/acs.analchem.5b03122, 2016a.
592
593 Alam, M. S., Zeraati-Rezaei, S., Stark, C. P., Liang, Z., Xu, H., and Harrison, R. M.: The
594 characterisation of diesel exhaust particles - composition, size distribution and partitioning,
595 Faraday. Discuss., 189, 69-84, http://www.doi.org/10.1039/C5FD00185D, 2016b.
596
597 Alam, M. S., Zeraati-Rezaei, S., Liang, Z., Stark, C., Xu, H., MacKenzie, A. R., and Harrison, R.
598 M.: Mapping and quantifying isomer sets of hydrocarbons (≥ C 12) in diesel exhaust, lubricating oil
599 and diesel fuel samples using GC× GC-ToF-MS, Atmos. Meas. Tech., 11, 3047,
600 https://doi.org/10.5194/amt-11-3047-2018, 2018.
601
602 Algrim, L. B., and Ziemann, P. J.: Effect of the Keto Group on yields and composition of organic
603 aerosol formed from OH radical-initiated reactions of ketones in the presence of NO_x, J. Phys.
604 Chem. A., 120, 6978-6989, http://www.doi.org/10.1021/acs.jpca.6b05839, 2016.
605
606 Alves, C., Pio, C., and Duarte, A.: Composition of extractable organic matter of air particles from
607 rural and urban Portuguese areas, Atmos. Environ., 35, 5485-5496, https://doi.org/10.1016/S1352-
608 2310(01)00243-6, 2001.
609
610 Andreou, G., and Rapsomanikis, S.: Origins of n-alkanes, carbonyl compounds and molecular
611 biomarkers in atmospheric fine and coarse particles of Athens, Greece, Sci. Total. Environ., 407,
612 5750-5760, http://dx.doi.org/10.1016/j.scitotenv.2009.07.019, 2009.
613
614 Aschmann, S. M., Arey, J., and Atkinson, R.: Atmospheric chemistry of three C10 alkanes, J. Phys.
615 Chem. A., 105, 7598-7606, http://www.doi.org/10.1021/jp010909j, 2001.
616
617 Bray, E., and Evans, E.: Distribution of n-paraffins as a clue to recognition of source beds,
618 Geochim. Cosmochim. Ac., 22, 2-15, https://doi.org/10.1016/0016-7037(61)90069-2, 1961.
619
620 Callen, M. S., de la Cruz, M. T., opez, J. M., Murillo, R., Navarro, M. V., and Mastral, A. M.:
621 Some inferences on the mechanism of atmospheric gas/particle partitioning of polycyclic aromatic
622 hydrocarbons (PAH) at Zaragoza (Spain), Chemosphere, 73, 1357-1365, 2008.
623
624 Chacon-Madrid, H., and Donahue, N.: Fragmentation vs. functionalization: chemical aging and
625 organic aerosol formation, Atmos. Chem. Phys., 11, 10553-10563, https://doi.org/10.5194/acp-11-
626 10553-2011, 2011.

627 Chacon-Madrid, H. J., Presto, A. A., and Donahue, N. M.: Functionalization vs. fragmentation: n-
628 aldehyde oxidation mechanisms and secondary organic aerosol formation, Phys. Chem. Chem.
629 Phys., 12, 13975-13982, http://www.doi.org/10.1039/C0CP00200C, 2010.
630 Cheng, Y., Li, S.-M., Leithead, A., and Brook, J. R.: Spatial and diurnal distributions of n-alkanes
631 and n-alkan-2-ones on PM 2.5 aerosols in the Lower Fraser Valley, Canada, Atmos. Environ., 40,
632 2706-2720, https://doi.org/10.1016/j.atmosenv.2005.11.066, 2006.
633
634 Cincinelli, A., Del Bubba, M., Martellini, T., Gambaro, A., and Lepri, L.: Gas-particle
635 concentration and distribution of *n*-alkanes and polycyclic aromatic hydrocarbons in the atmosphere
636 of Prato (Italy), Chemosphere, 68, 472-478, 2007.
637
638 Duan, H., Liu, X., Yan, M., Wu, Y., and Liu, Z.: Characteristics of carbonyls and volatile organic
639 compounds (VOCs) in residences in Beijing, China, Front. Env. Sci. Eng., 10, 73-84,
640 http://www.doi.org/10.1007/s11783-014-0743-0, 2016.
641
642 Gentner, D. R., Worton, D. R., Isaacman, G., Davis, L. C., Dallmann, T. R., Wood, E. C., Herndon,
643 S. C., Goldstein, A. H., and Harley, R. A.: Chemical composition of gas-phase organic carbon
644 emissions from motor vehicles and implications for ozone production, Environ. Sci. technol., 47,
645 11837-11848, http://www.doi.org/10.1021/es401470e, 2013.
646
647 Gogou, A., Stratigakis, N., Kanakidou, M., and Stephanou, E. G.: Organic aerosols in Eastern
648 Mediterranean: components source reconciliation by using molecular markers and atmospheric back
649 trajectories, Org. Geochem., 25, 79-96, https://doi.org/10.1016/S0146-6380(96)00105-2, 1996.
650
651 Han, Y., Kawamura, K., Chen, Q., and Mochida, M.: Formation of high-molecular-weight
652 compounds via the heterogeneous reactions of gaseous C8–C10 n-aldehydes in the presence of
653 atmospheric aerosol components, Atmos. Environ., 126, 290-297,
654 http://dx.doi.org/10.1016/j.atmosenv.2015.11.050, 2016.
655
656 Harrison, R., Dall'Osto, M., Beddows, D., Thorpe, A., Bloss, W., Allan, J., Coe, H., Dorsey, J.,
657 Gallagher, M., and Martin, C.: Atmospheric chemistry and physics in the atmosphere of a
658 developed megacity (London): an overview of the REPARTEE experiment and its conclusions,
659 Atmos. Chem. Phys., 12, 3065-3114, https://doi.org/10.5194/acp-12-3065-2012, 2012.
660
661 Harrison, R. M., and Beddows, D. C.: Efficacy of recent emissions controls on road vehicles in
662 Europe and implications for public health, Sci. Rep-UK., 7, 1152,
663 http://www.doi.org/10.1038/s41598-017-01135-2., 2017.
664
665 Karanasiou, A. A., Sitaras, I. E., Siskos, P. A., and Eleftheriadis, K.: Size distribution and sources
666 of trace metals and *n*-alkanes in the Athens urban aerosol during summer, Atmos. Environ., 41,
667 2368-2381, 2007.
668
669 Kwok, E. S., and Atkinson, R.: Estimation of hydroxyl radical reaction rate constants for gas-phase
670 organic compounds using a structure-reactivity relationship: an update, Atmos. Environ., 29, 1685-
671 1695, https://doi.org/10.1016/1352-2310(95)00069-B, 1995.

Lim, Y. B., and Ziemann, P.J.: Chemistry of secondary organic aerosol formation from OH radical-initiated reactions of linear, branched, and cyclic alkanes in the presence of NO_x, Aerosol Sci. Technol., 43, 604-619, https://doi.org/10.1080/02786820902802567, 2009.

Liu, D., Allan, J., Young, D., Coe, H., Beddows, D., Fleming, Z., Flynn, M., Gallagher, M., Harrison, R., and Lee, J.: Size distribution, mixing state and source apportionments of black carbon aerosols in London during winter time, Atmos. Chem. Phys., 14, https://doi.org/10.5194/acp-14-10061-2014, 2014.

Ma, W.-L., Sun, D.-Z., Shen, W.-G., Yang, M., Qi, H., Liu, L.-Y., Shen, J.-M., and Li, Y.-F.: Atmospheric concentrations, sources and gas-particle partitioning of PAHs in Beijing after the 29th Olympic Games, Environ. Pollut., 159, 1794-1801, 2011.

Mandalakis, M., Tsapakis, M., Tsoga, A., and Stephanou, E. G.: Gas-particle concentrations and distribution of aliphatic hydrocarbons, PAHs, PCBs and PCDD/Fs in the atmosphere of Athens (Greece), Atmos. Environ., 36, 4023-4034, 2002.

Oliveira, T. S., Pio, C., Alves, C. A., Silvestre, A. J., Evtyugina, M., Afonso, J., Fialho, P., Legrand, M., Puxbaum, H., and Gelencsér, A.: Seasonal variation of particulate lipophilic organic compounds at nonurban sites in Europe, J. Geophys. Res-Atmos., 112, https://doi.org/10.1029/2007JD008504 2007.

Oros, D. R., and Simoneit, B. R. T.: Identification and emission rates of molecular tracers in coal smoke particulate matter, Fuel., 79, 515-536, http://dx.doi.org/10.1016/S0016-2361(99)00153-2, 2000.

Pankow, J. F.: An absorption model of gas/particle partitioning of organic compounds in the atmosphere, Atmos. Environ., 28, 185-188, https://doi.org/10.1016/1352-2310(94)90093-0, 1994.

Perrone, M. G., Carbone, C., Faedo, D., Ferrero, L., Maggioni, A., Sangiorgi, G., and Bolzacchini, E.: Exhaust emissions of polycyclic aromatic hydrocarbons, n-alkanes and phenols from vehicles coming within different European classes, Atmos. Environ., 82, 391-400, https://doi.org/10.1016/j.atmosenv.2013.10.040, 2014.

Rogge, W. F., Hildemann, L. M., Mazurek, M. A., and Cass, G. R.: Sources of fine organic aerosol. 9. Pine, oak, and synthetic log combustion in residential fireplaces, Environ. Sci. Technol., 32, 13-22, http://www.doi.org/10.1021/es960930b, 1998.

Ruehl, C. R., Nah, T., Isaacman, G., Worton, D. R., Chan, A. W. H., Kolesar, K. R., Cappa, C. D., Goldstein, A. H., and Wilson, K. R.: The influence of molecular structure and aerosol phase on the heterogeneous oxidation of normal and branched alkanes by OH, J. Phys. Chem. A., 117, 3990-4000, http://www.doi.org/10.1021/jp401888q, 2013.

Schauer, J. J., Kleemanm M. J., Cass, G. R., and Simoneit, B. R. T.: Measurement of emissions from air pollution sources. 2. C1 through C30 organic compounds from medium duty diesel trucks, Environ. Sci.Technol., 33, 1578-1587, 10.1021/es980081n, 1999a.

Schauer, J. J., Kleeman, M. J., Cass, G. R., and Simoneit, B. R. T.: Measurement of emissions from air pollution sources. 1. C1 through C29 organic compounds from meat charbroiling, Environ. Sci. Technol., 33, 1566-1577, http://www.doi.org/10.1021/es980076j, 1999b.

Schauer, J. J., Kleeman, M. J., Cass, G. R., and Simoneit, B. R. T.: Measurement of emissions from air pollution sources. 3. C1−C29 organic compounds from fireplace combustion of wood, Environ. Sci. technol., 35, 1716-1728, http://www.doi.org/10.1021/es001331e, 2001.

Schauer, J. J., Kleeman, M. J., Cass, G. R., and Simoneit, B. R. T.: Measurement of emissions from air pollution sources. 4. C1−C27 organic compounds from cooking with seed oils, Environ. Sci. Technol., 36, 567-575, http://www.doi.org/10.1021/es002053m, 2002a.

Schauer, J. J., Kleeman, M. J., Cass, G. R., and Simoneit, B. R. T.: Measurement of emissions from air pollution sources. 5. C1−C32 organic compounds from gasoline-powered motor vehicles, Environ. Sci. Technol., 36, 1169-1180, http://www.doi.org/10.1021/es0108077, 2002b.

Schilling Fahnestock, K. A., Yee, L. D., Loza, C. L., Coggon, M. M., Schwantes, R., Zhang, X., Dalleska, N. F., and Seinfeld, J. H.: Secondary organic aerosol composition from C12 alkanes, J. Phys. Chem. A., 119, 4281-4297, http://www.doi.org/10.1021/jp501779w, 2015.

Simoneit, B. R. T., Cox, R. E., and Standley, L. J.: Organic matter of the troposphere - IV. Lipids in harmattan aerosols of Nigeria, Atmos. Environ., 22, 983-1004, https://doi.org/10.1016/0004-6981(88)90276-4, 1967.

UK-Air, https://uk-air.defra.gov.uk, last accessed 16 December 2018.

Wang, W., Massey Simonich, S. L., Wang, W., Giri, B., Zhao, J., Xue, M., Cao, J., Lu, X. and Tao, S.: Atmospheric polycyclic aromatic hydrocarbon concentrations and gas/paticle partitioning at background, rural village and urban sites in the North China Plain, Atmos. Res., 99, 197-206, 2011.

Yee, L. D., Craven, J. S., Loza, C. L., Schilling, K. A., Ng, N. L., Canagaratna, M. R., Ziemann, P. J., Flagan, R. C., and Seinfeld, J. H.: Secondary organic aerosol formation from low-NO_x photooxidation of dodecane: Evolution of multigeneration gas-phase chemistry and aerosol composition, J. Phys. Chem. A., 116, 6211-6230, http://www.doi.org/10.1021/jp211531h, 2012.

Zhang, H., Worton, D. R., Shen, S., Nah, T., Isaacman-VanWertz, G., Wilson, K. R., and Goldstein, A. H.: Fundamental time scales governing organic aerosol multiphase partitioning and oxidative aging, Environ. Sci. technol., 49, 9768-9777, http://www.doi.org/10.1021/acs.est.5b02115, 2015.

760 Zhao, Y., Hu, M., Slanina, S., and Zhang, Y.: The molecular distribution of fine particulate organic
761 matter emitted from Western-style fast food cooking, Atmos. Environ., 41, 8163-8171,
762 http://dx.doi.org/10.1016/j.atmosenv.2007.06.029, 2007a.
763
764 Zhao, Y., Hu, M., Slanina, S., and Zhang, Y.: Chemical compositions of fine particulate organic
765 matter emitted from Chinese cooking, Environ. Sci. Technol., 41, 99-105,
766 http://www.doi.org/10.1021/es0614518, 2007b.
767
768 Ziemann, P. J.: Effects of molecular structure on the chemistry of aerosols formation from the
769 OH-radical-initiated oxidation of alkanes and alkenes, Intl. Rev. Phys. Chem., 30, 161-195,
770 https://doi.org/10.1080/0144235X.2010.550728, 2011.
771
772
773

TABLE LEGENDS

Table 1. The carbon preference index (CPI) and C_{max} for n-alkanals, n-alkan-2-ones, and n-alkan-3-ones in this study and published data.

Table 2. Percentages of particle phase form and the partitioning coefficient Kp.

FIGURE LEGENDS

Figure 1. Map of the sampling sites. RU-Regents University (15 m above ground); WM-University of Westminster (20 m above ground); EL-Eltham; MR-Marylebone Road (south side).

Figure 2. Time series of particle-bound ∑n-alkanals, ∑n-alkan-2-ones and ∑n-alkan-3-ones at RU, WM, EL, and MR sites.

Figure 3. The average total concentration of particle-bound n-alkanals (C_8-C_{20}), n-alkan-2-ones (C_8-C_{26}), and n-alkan-3-ones (C_8-C_{19}), for each sampling period and site. The error bars indicate one standard deviation.

Figure 4. The molecular distribution of particle-bound carbonyl compounds at four sites (RU, WM, EL, and MR).

Table 1. The carbon preference index (CPI) and C_{max} for n-alkanals, n-alkan-2-ones, and n-alkan-3-ones in this study and published data.

Location	Sampling period	n-alkanals		n-alkan-2-ones		n-alkan-3-ones		Reference
Sampling site		CPI	C_{max}	CPI	C_{max}	CPI	C_{max}	
RU, surrounded by Regent's Park, 15 m above ground	23 Jan - 19 Feb	0.52	C_8	1.23	C_{19}	1.30	C_{17}	Present study
WM, 20 m above ground	24 Jan - 20 Feb	0.41	C_8	0.99	C_{20}	1.26	C_{17}	Present study
EL, suburb of London	23 Feb - 21 Mar	0.71	C_8	1.57	C_{20}	1.04	C_{16}	Present study
MR, adjacent to Marylebone road	22 Mar - 18 Apr	1.07	C_8	0.57	C_{16}	1.12	C_{16}	Present study
Athens, Athinas St.	August	1.49	C_{15}, C_{17}	1.09	C_{18}, C_{21}, C_{19}			(Andreou and
Urban roadside	March			3.26	C_{21}, C_{19}, C_{20}			Rapsomanikis, 2009)
Athens, AEDA, Urban, 20 m above ground	March			2.41	C_{19}, C_{18}, C_{20}			(Andreou and Rapsomanikis, 2009)
Heraklion, Greece Urban 15 m above ground	Spring /summer	0.80–1.40	C_{26}, C_{28}	1.30–1.80	C_{23}, C_{29}, C_{31}			(Gogou et al., 1996)
Vancouver, Canada Roadway tunnel				1.33	C_{17}, C_{19}			(Cheng et al., 2006)
Aveiro, Portugal	Summer		C_{22}, C_{23}, C_{26}		C_{26}, C_{28}, C_{30}			
Suburban	Winter							(Oliveira et al., 2007)
K-Puszta, Hungary	Summer		C_{24}, C_{26}, C_{28}		C_{24}, C_{26}, C_{28}			

Table 2. Percentages of particle phase form and the partitioning coefficient Kp (m^3 μg^{-1}).

	RU						WM					
	n-alkanals		n-alkan-2-ones		n-alkan-3-ones		n-alkanals		n-alkan-2-ones		n-alkan-3-ones	
	%	Kp	%	Kp	%	Kp	%	Kp	%	Kp	%	Kp
C_8	82.9	1.16E-04	18.4	5.37E-06	23.9	7.47E-06	80.2	9.09E-05	13.3	3.43E-06	34.1	1.16E-05
C_9	69.2	5.37E-05	14.5	4.03E-06	16.6	4.74E-06	60.5	3.43E-05	15.6	4.16E-06	28.7	9.05E-06
C_{10}	75.3	7.27E-05	13.6	3.77E-06	7.43	1.92E-06	82.1	1.03E-04	14.4	3.77E-06	23.3	6.82E-06
C_{11}	45.5	1.99E-05	21.4	6.49E-06	12.8	3.49E-06	62.4	3.72E-05	20.1	5.65E-06	36.3	1.28E-05
C_{12}	74.8	7.08E-05	25.0	7.96E-06	31.3	1.09E-05	73.7	6.29E-05	28.8	9.07E-06	22.7	6.60E-06
C_{13}	82.9	1.15E-04	61.0	3.74E-05	35.4	1.31E-05	82.2	1.04E-04	48.9	2.14E-05	62.5	3.74E-05
C_{14}	82.8	1.15E-04	49.5	2.34E-05	35.5	1.31E-05	75.8	7.04E-05	31.8	1.05E-05	25.6	7.74E-06
C_{15}	99.5	5.01E-03	84.1	1.26E-04	50.5	2.44E-05	*		85.0	1.27E-04	68.5	4.87E-05
C_{16}	*		91.4	2.53E-04	70.3	5.64E-05	*		89.6	1.93E-04	91.7	2.47E-04
C_{17}	*		91.5	2.55E-04	*		*		85.9	1.36E-04	91.5	2.42E-04
C_{18}	*		94.1	3.80E-04	*		*		84.8	1.26E-04	99.4	4.02E-03
C_{19}	*		99.1	2.69E-03			*		*			
C_{20}	*		*				*		*			
C_{21}			*						*			
C_{22}			*						*			
C_{23}			*						*			
C_{24}			*						*			
C_{25}			*						*			
C_{26}			*						*			

	El						MR					
	n-alkanals		n-alkan-2-ones		n-alkan-3-ones		n-alkanals		n-alkan-2-ones		n-alkan-3-ones	
	%	Kp	%	Kp	%	Kp	%	Kp	%	Kp	%	Kp
C_8	92.7	6.53E-04	24.9	1.72E-05	31.9	2.43E-05	90.0	2.94E-04	28.2	1.28E-05	43.0	2.46E-05
C_9	92.2	6.16E-04	38.0	3.18E-05	44.4	4.15E-05	89.9	2.89E-04	27.0	1.20E-05	39.1	2.09E-05
C_{10}	90.5	4.96E-04	47.6	4.70E-05	47.0	4.59E-05	91.7	3.62E-04	61.1	5.12E-05	20.4	8.33E-06
C_{11}	87.0	3.47E-04	72.3	1.35E-04	81.9	2.34E-04	87.4	2.26E-04	50.2	3.28E-05	33.1	1.61E-05
C_{12}	92.9	6.73E-04	83.4	2.60E-04	66.4	1.02E-04	93.0	4.30E-04	88.5	2.51E-04	28.1	1.28E-05
C_{13}	95.6	1.12E-03	82.2	2.40E-04	65.7	9.92E-05	96.1	8.04E-04	87.7	2.33E-04	46.2	2.79E-05
C_{14}	91.4	5.52E-04	90.3	4.80E-04	59.1	7.48E-05	95.2	6.51E-04	95.9	7.61E-04	72.0	8.38E-05
C_{15}	96.7	1.53E-03	94.5	8.98E-04	84.4	2.80E-04	*		96.9	1.02E-03	83.8	1.69E-04
C_{16}	*		96.7	1.41E-03	89.0	4.18E-04	*		96.4	8.70E-04	88.0	2.38E-04
C_{17}	*		95.1	1.00E-03	81.5	2.28E-04	*		96.0	7.73E-04	88.0	2.39E-04
C_{18}	*		64.6	9.44E-05	85.0	2.93E-04	*		92.5	4.04E-04	*	
C_{19}	*		*				*		*		*	
C_{20}	*		*				*		*			
C_{21}			*						*			
C_{22}			*						*			
C_{23}			*						*			
C_{24}									*			

* For compounds marked with an asterisk, the particulate phase was quantified, but the vapour was below detection limit, and hence K_p is undefined.

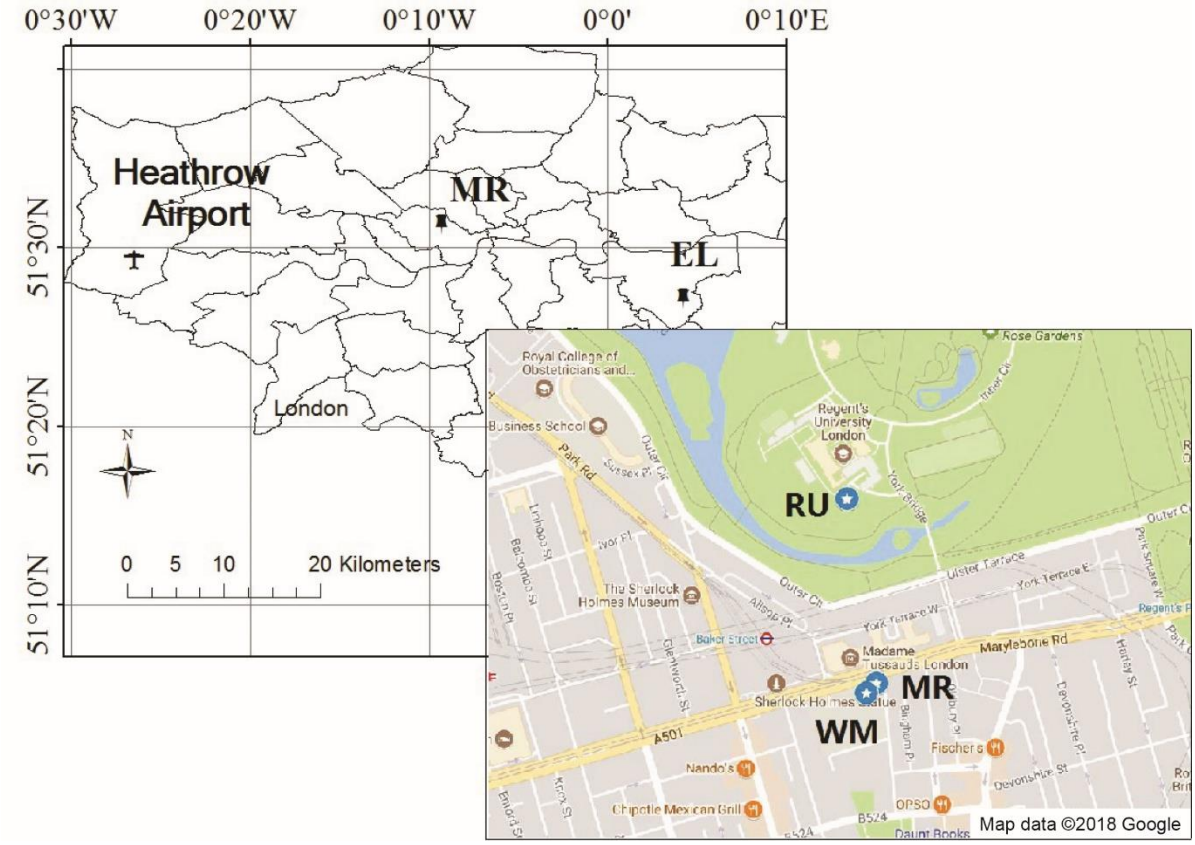

Fig. 1. Map of the sampling sites. RU-Regents University (15 m above ground); WM-University of Westminster (20 m above ground); EL-Eltham; MR-Marylebone Road (south side).

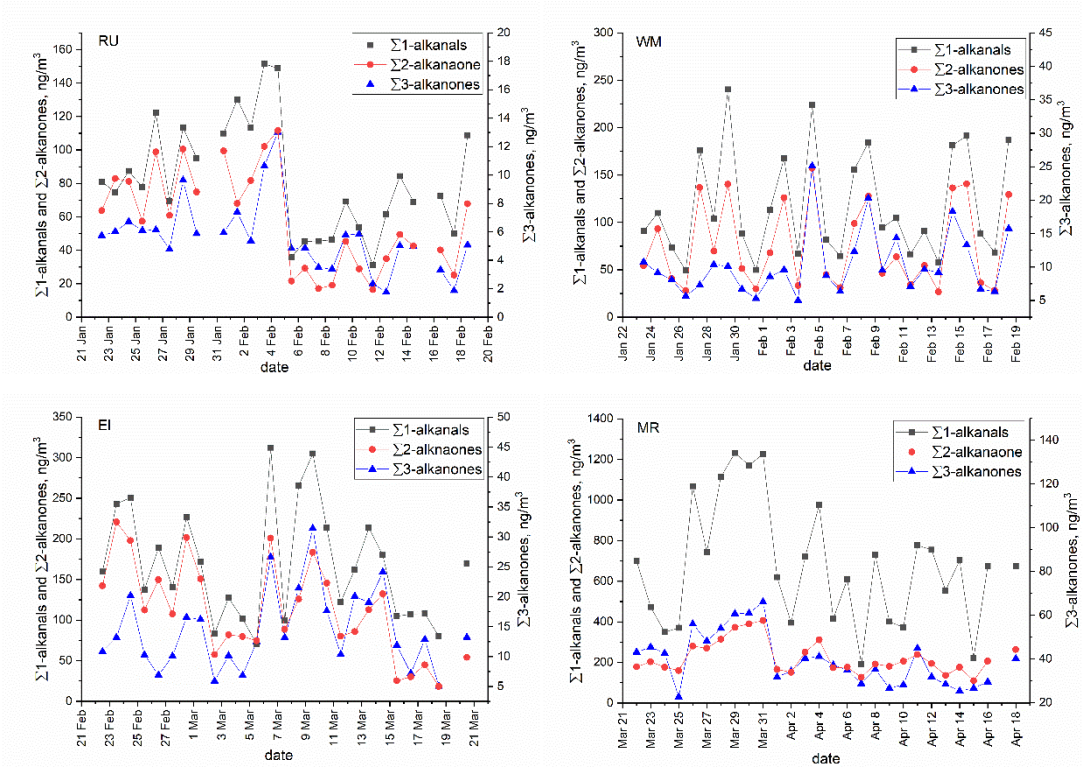

Fig. 2. Time series of particle-bound ∑n-alkanals, ∑n-alkan-2-ones and ∑n-alkan-3-ones at RU, WM, EL, and MR sites.

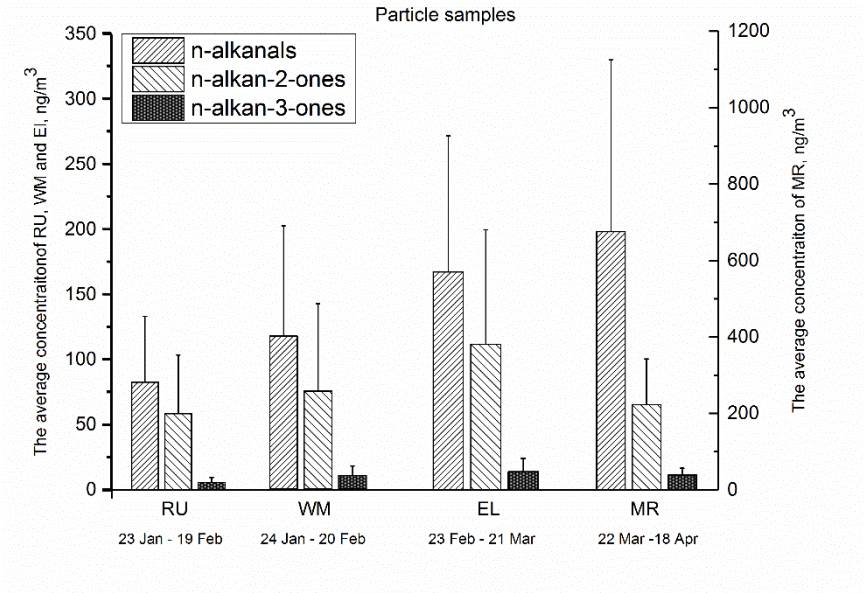

Fig. 3. The average total concentration of particle-bound n-alkanals (C_8-C_{20}), n-alkan-2-ones (C_8-C_{26}), and n-alkan-3-ones (C_8-C_{19}), for each sampling period and site. The error bars indicate one standard deviation.

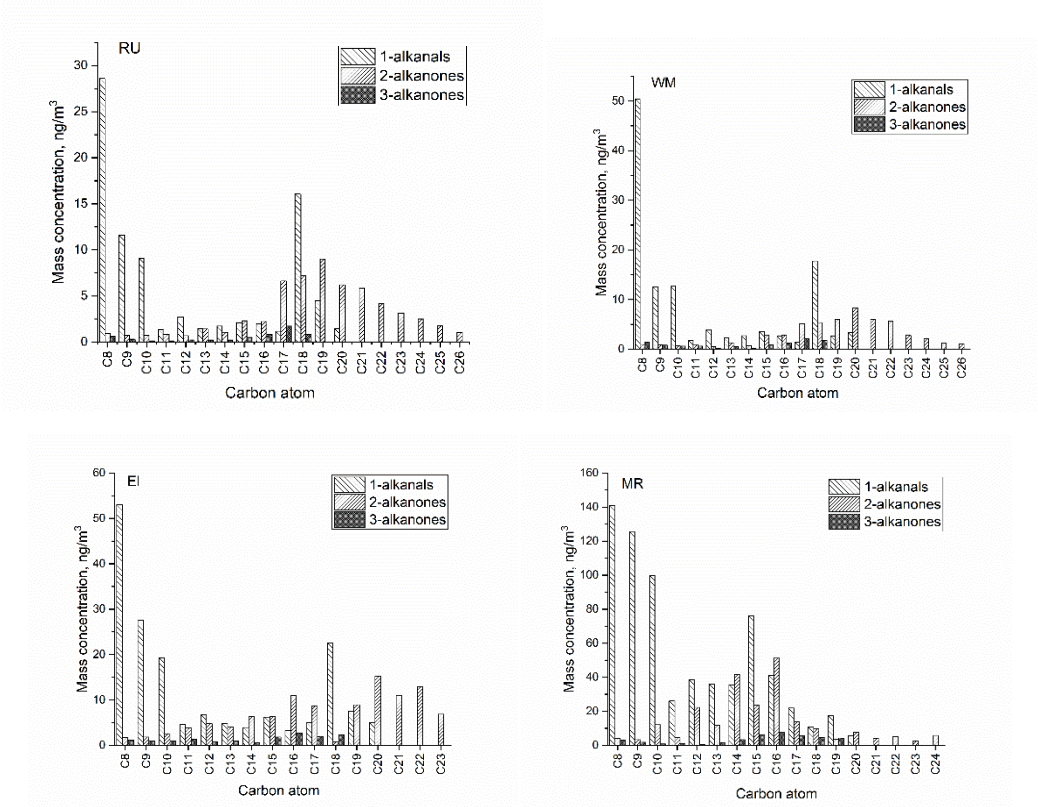

Fig. 4. The molecular distribution of particle-bound carbonyl compounds at four sites (RU, WM, EL, and MR).